BOREAL ENVIRONMENT RESEARCH 20: 196–212
ISSN 1239-6095 (print) ISSN 1797-2469 (online)

Helsinki 30 April 2015

Consistent estimates of gross primary production of Finnish forests — comparison of estimates of two process models

Mikko Peltoniemi[1)]*, Tiina Markkanen[2)], Sanna Härkönen[3)], Petteri Muukkonen[1)], Tea Thum[2)], Tuula Aalto[2)] and Annikki Mäkelä[4)]

[1)] *Finnish Forest Research Institute (METLA), P.O. Box 18, FI-01301 Vantaa, Finland (*corresponding author' e-mail: mikko.peltoniemi@metla.fi)*
[2)] *Finnish Meteorological Institute, P.O. Box 503, FI-00101 Helsinki, Finland*
[3)] *Finnish Forest Research Institute (METLA), P.O. Box 68, FI-80101 Joensuu, Finland*
[4)] *Department of Forest Sciences, P.O. Box 27, FI-00014 University of Helsinki, Finland*

Received 26 Nov. 2013, final version received 9 Oct. 2014, accepted 9 Oct. 2014

Peltoniemi M., Markkanen T., Härkönen S., Muukkonen P., Thum T., Aalto T. & Mäkelä A. 2015: Consistent estimates of gross primary production of Finnish forests — comparison of estimates of two process models. *Boreal Env. Res.* 20: 196–212.

We simulated Gross Primary Production (GPP) of Finnish forests using a landsurface model (LSM), JSBACH, and a semi-empirical stand-flux model PRELES, and compared their predictions with the MODIS GPP product. JSBACH used information about plant functional type fractions in 0.167° pixels. PRELES applied inventory-scaled information about forest structure at high resolution. There was little difference between the models in the results aggregated to national level. Temporal trends in annual GPPs were also parallel. Spatial differences could be partially related to differences in model input data on soils and leaf area. Differences were detected in the seasonal pattern of GPP but they contributed moderately to the annual totals. Both models predicted lower GPPs than MODIS, but MODIS still showed similar south–north distribution of GPP. Convergent results for the national total GPP between JSBACH and PRELES, and those derived for comparison from the forest ghg-inventory, implied that modelled GPP estimates can be realistically upscaled to larger region in spite of the fact that model calibrations may not originate from the study region, or that a limited number of sites was used in the calibration of a model.

Introduction

Vegetation is in continuous interaction with the atmosphere. This interaction is incorporated into weather prediction and climate models by means of land surface models (LSM) describing the material and energy fluxes between the atmosphere, vegetation and soils (Bonan 2008). For predictions of the present-day climate, the role of the LSM is to provide a reliable energy balance, accounting for both radiation and the turbulent fluxes of energy. Earth system models (ESM) targeted for climate scenarios extending over decades or centuries also require that the LSMs describe the whole carbon cycle with its links to the nutrient and hydrological cycles (Friedlingstein *et al*. 2006). These models are largely based on our mechanistic and theoretical understanding of how vegetation regulates the material fluxes, and *vice versa*, how climate molds the type and density of vegetation. The widening eddy-flux network has increasingly been used

Editor in charge of this article: Eero Nikinmaa

for model parameterisation and testing (Williams *et al*. 2009, Jung *et al*. 2011).

When a vegetation model is integrated into a climate modelling scheme, some simplifying assumptions are made to compensate for a lack of empirical information. A key assumption in most LSMs is that the ecosystem is in a steady state regarding its vegetation type and biomass The vegetation type is usually defined in terms of plant functional type (PFT), such as needle-leaved evergreen or broad-leaved summergreen (Prentice *et al*. 1992). Past land covers and corresponding PFT distributions have typically been implemented by means of a series of prescribed PFT distribution maps based on knowledge on historical land cover changes (Brovkin *et al*. 2006, Williams *et al*. 2009, Pongratz *et al*. 2009, Pongratz *et al*. 2010). The steady-state assumption is practical when no information is available about forest management or natural disturbance regimes, but is likely to be seriously violated if these regimes involve intensive disturbances from the steady state. Work is currently underway to incorporate both forest management and disturbance modules in LSMs (Bellassen *et al*. 2010). Moreover, LSMs are being developed to account for the impact of climate change on global PFT distributions (e.g. Reick *et al*. 2013).

While it is necessary for future climate projections that ESMs produce both vegetation and climate variables as a result of model internal dynamics, a more simple, "feed-forward" approach where forest structure and climate variables are input from measurements to flux models, is sufficient for monitoring current fluxes from the vegetation. Perhaps the best-known application of this approach are the MODIS-derived GPP and NPP, which are based on a daily light-use-efficiency model of net photosynthetic production and satellite-driven information about leaf area. MODIS-based NPP has been found to be an overestimate particularly in low productivity sites and in managed forests (Hasenauer *et al*. 2012). However, the light-use efficiency (LUE) based approach has recently been under further development to represent better the annual cycle of the boreal forest (Mäkelä *et al*. 2008, Peltoniemi *et al*. 2015).

Information about forest structure is required as input to the "feed-forward" models, but it would also be very helpful for LSMs as regards model development, validation and uncertainty analysis. While the MODIS products are based on satellite data, a comparison with ground-based estimates could improve the confidence of the predictions (Härkönen *et al*. 2015). Many countries have established forest inventories which provide representative sampling of forests. Inventories apply ground reference plot information and aerial and satellite images to scale point measurements to wall-to-wall mapping of forest resources (Poso 1972, Kilkki and Päivinen 1987, Tomppo 1990), with nearest-neighbour methods that originate from the study on non-parametric pattern recognition (Fix and Hodges 1951). Operative forest inventories quickly adopted and further developed these ideas (Tomppo *et al*. 2008). At present, forest inventory maps are routinely produced, and owing to the INSPIRE directive set by the EU (EC 2007), they are now publicly available in all EU countries. Such information has reinforced concurrent biomass mapping (Tuominen *et al*. 2010), and it can directly benefit forest carbon balance estimation (Härkönen *et al*. 2011). Inventories also offer a valuable source of information for testing LSMs with respect to their predictions of forest biomass, LAI and GPP.

In this study, we utilise ground-based forest inventory data and three different approaches applying different parametrizations and input data to estimate GPP of forests in Finland. The approaches include (1) JSBACH (Raddatz *et al*. 2007, Reick *et al*. 2013) which is LSM of the ECHAM6 climate model (Stevens *et al*. 2013), and is now being applied in Finland with the REMO regional climate model (Jacob and Podzun 1997, Jacob 2001) with spatial resolution of approximately 18 km; (2) PRELES, an eddy-flux-based semiempirical GPP and water-balance model (Peltoniemi *et al*. 2015) requiring forest structure data and meteorological measurements as input; and (3) GPP derived from MODIS satellite-based input data of forest LAI and meteorological variables (Running *et al*. 2004, Zhao *et al*. 2005, Zhao *et al*. 2006). The objective was to screen the total annual production and its temporal and spatial distribution in the approaches, so as to analyse the causes of possible discrepancies between the models. Especially, we aimed to assess to what degree

the possible differences are related to either forest structure or to the response of GPP to climate in the models.

Material and methods

Below, we describe two model approaches taken to estimate GPP of Finnish forests which are different regarding modelling approach, model structure and input data. MODIS GPP is available as a product and will not be described in detail here (*see* Running *et al*. 2004, Zhao *et al*. 2005, Zhao *et al*. 2006).

Models and model implementations

JSBACH

In JSBACH, land surface is a fractional structure where the land grid-cells are divided into tiles representing the most prevalent PFTs within each grid cell (Raddatz *et al*. 2007, Reick *et al*. 2013). Runs for this work were conducted with four tiles per grid cell. PFTs are characterized by a set of parameters that control vegetation related biological and physical processes accounting for the land–atmosphere interactions.

For our regional application, we adopted the land cover information from European Corine Landcover (CLC) (Büttner and Kosztra 2007). CLC data are first allocated to Olson (Olson 1994a, 1994b) land-cover classes (Gao *et al*. 2015) and then aggregated into prescribed current PFTs using the translation rules (Table 1). The two translations yielded fractional coverages of 77% and 23% for coniferous-evergreen trees and temperate-broadleaf deciduous trees, respectively.

The seasonal development of LAI is regulated by air temperature and soil moisture with PFT specific maximum LAI as a limiting value. For generation of the seasonal cycle, PFTs are divided into the following phenology types: summergreen, evergreen, grass and crop. Soil moisture is not taken into account in summergreen and evergreen phenologies, to which northern forests belong, but their seasonal development is driven solely by pseudo soil temperature that is a weighted running mean of air temperature. Potential GPP of summergreen PFT is constrained by phenology, namely their leaf onset and shedding. In the case of Evergreen Boreal Forest, the phenology model produces periods of growth and rest, each having LAI greater than zero. The predictions of phenology are produced by the phenology model of JSBACH (LoGro-P), which has altogether 10 to 20 phenology type specific parameters including shedding and growth rates and critical temperatures. The maximum leaf area of Finnish forest PFTs, temperate broadleaf deciduous trees and coniferous evergreen trees, is set to 5.0 m^2 m^{-2}.

Photosynthesis of trees, is described with the biochemical photosynthesis model (Farquhar *et al*. 1980), which has two PFT-specific parameters in JSBACH; V_{max} giving maximum carboxylation rate in and J_{max} for maximum electron transport rate. A systematic analysis of a broad measurement database determined by means of data assimilation revealed a relationship between nitrogen use efficiency and V_{max} per PFT (Kattge *et al*. 2009). The values used in this study are global and as JSBACH is run without explicit nitrogen cycle, the mean values of V_{max} were applied. J_{max} is set to a typical value of $1.9V_{max}$ for all PFTs (Wullschleger 1993, Kattge *et al*. 2009).

The photosynthetic rate is resolved in two steps in hourly time steps. First stomatal con-

Table 2. Translation rules between CORINE, Olson's classification and PFTs in JSBACH. Only the forest types existing in Finland are included in the table.

Corine Land Cover class	Olson's class	PFT
3.1.1 Broad-leaved forest	25 Cool Broadleaf Forest	Temperate broadleaf deciduous trees
3.1.2 Coniferous forest	21 Conifer Boreal Forest	Coniferous evergreen trees
3.1.3 Mixed forest	23 Cool Mixed Forest	50% Temperate broadleaf deciduous trees 50% Coniferous evergreen trees

ductance under non-water-stressed conditions is assumed to be controlled by photosynthetic activity (Schulze *et al*. 1994). The leaf internal CO_2 concentration is assumed to be a constant fraction of ambient concentration which allows for an explicit resolution of the photosynthesis (*see* e.g. Knorr 1997). Finally, the impact of soil water availability is accounted for by a soil moisture dependent multiplier that is identical for each canopy layer (Knorr 1997).

Radiation absorption was estimated with three-layer canopy, and the scheme for radiation inside the canopy uses a two-stream approximation (Sellers 1985). Especially in the sparse canopies the radiation absorption is affected by clumping of the leaves acording to the formulation by Knorr (1997).

We applied a new five-layer soil moisture scheme (Hagemann and Stacke 2015) in which the soil information is not merely PFT specific but partly based on soil texture data. The soil water holding capacity varies according to fractions of land-cover classes in each grid cell (Hagemann 2002) while other soil information are based on soil texture data obtained from a global soil map (FAO 1979). Soil texture types present in Finland were: peat, loamy sand, clay and coarse. Values of seven soil parameter values required by the new soil model are given elsewhere (Hagemann and Stacke 2015). As the resolution of the soil texture data is 0.5°, the parameter values are interpolated to the present grid of 0.167° resolution. Finally, rooting depth is calculated from the total soil water holding capacity and a FAO soil type dependent parameter volumetric field capacity (FAO 1979).

We ran JSBACH with hourly climatic forcing for a study area and a resolution that is higher than its resolution in the context of MPI-ESM (Reick *et al*. 2013). No additional regional or site level calibrations of the model parameters were conducted for this study, instead the global PFT-specific values are applied. For comparison of forest GPPs we extracted the values corresponding forest PFT tiles of each grid cell.

PRELES

PRELES is a semi-empirical model of forest GPP and water fluxes. The model essentially treats the canopy as a big leaf, and it operates at a daily resolution. The model applies a light-use efficiency concept (developed for NPP by Monteith and Moss 1977) for GPP. In this approach, there is a potential light-use efficiency that is scaled down in suboptimal environmental conditions for photosynthesis. These scaling factors are environmental '*f*-modifiers' and they are between 0 and 1. Similar approach of multiplicative constraints has been applied in many GPP models, such as Cfix (Veroustraete *et al*. 2002), VPM (Xiao *et al*. 2004) and MODIS GPP product. Our approach to estimating GPP is based on Mäkelä *et al*. (2008), and it has been modified by Peltoniemi *et al*. (2015) to include a simplified representation of stand water-budget.

The model has *f*-modifiers for light (f_L), vapour pressure deficit (f_D), temperature acclimation (f_S), and fraction of absorbed photosynthetic photon flux density ($f_{a\phi}$). There is also a *f*-modifier for for soil water that is estimated with a one-pool model (Peltoniemi *et al*. 2015). Soil water is affected by evapotranspiration estimated with an empirical function applying GPP prediction and parameters associated with transpiration efficiency. The model also includes pools of snow water and a surface water storage, which is affected by LAI. The model has recently been calibrated to eddy-covariance sites in Hyytiälä and Sodankylä. The model, the calibration and a model's sensitivity analysis are described in Peltoniemi *et al*. (2015).

Forest data for PRELES were based on the national forest inventory data (NFI) of Finland (Tomppo *et al*. 2012). The fraction of absorbed photosynthetic photon flux density ($f_{a\phi}$) was estimated for each forest-inventory plot using foliage biomass models (Repola 2009), specific leaf area of different species (Härkönen *et al*. 2015), and a light extinction model with species-specific effective light extinction coefficients (Härkönen *et al*. 2010). Wall-to-wall estimates of $f_{a\phi}$ at 30-m resolution were obtained using *k*-nearest-neighbour (*k*NN) imputation based on the Landsat 5 TM satellite image bands 1–5 and 7 for forests (Härkönen *et al*. 2015).

Forest input data for simulations were further resampled to simulation units of 100 × 100 m, to reduce the random variation inherent in single

pixel (30 m) estimates, which typically have a relative root mean square error (RMSE) of 50% (Härkönen *et al*. 2015). Assuming uncorrelated neighbouring pixels thus would lead to 15% relative RMSE of 100 × 100 m pixels. A land-use map (30 m resolution) from multi-source NFI in 2007 (Tomppo *et al*. 2008, Tomppo *et al*. 2012) was utilized for calculating proportions of land use classes 1 and 2 in the simulation data. According to the Finnish NFI classification the land-use class 1 (*metsämaa* in Finnish) includes forests, with G of at least 1 m^3 ha^{-1} a^{-1} during a normal rotation length (in practice 1–8 m^3 ha^{-1} a^{-1}) (VMI 2008). Land-use class 2 (*kitumaa* in Finnish) contains a poorly-productive forest land, with mean growth (G) of only 0.1–0.99 m^3 ha^{-1} a^{-1}, The $f_{a\phi}$ map was applied in PRELES simulations for the land-use class 1 in each pixel, but not for land-use class 2 because there were not enough data for the imputations as described by Härkönen (2015). This underlines the small role of land-use class 2 in national total growth and GPP. Therefore, for land-use class 2, we used a fixed $f_{a\phi} = 0.35$, providing a rough estimate of the land area but with a small role in the national GPP total. This estimate of $f_{a\phi}$ was based on assumed average (all-sided) LAI = 2 m^2 m^{-2} and Scots pine light extinction coefficient that we estimated from the inventory data as an average for this land-use class with the methods presented above. Land-use class 2 covers 2.5% of the growing stock, although it covers 11% of the area (9% when unproductive land is included, G < 0.1 m^3 ha^{-1} a^{-1}) (Ylitalo 2012). These proportions increase towards northern Finland further decreasing the effect on national total GPP. The northernmost Finland was excluded from the result maps.

In the simulations, tree species differed in their potential LUE. The estimate of potential LUE of pines was LUE of Hyytiälä (Peltoniemi *et al*. 2015). Spruce and deciduous species LUEs were predicted assuming a linear relationship between LUE and mean foliar N concentration (Peltoniemi *et al*. 2012). In the samples collected from intensively monitored ecosystem sites in Finland, the mean N concentrations were 1.18 mg (g DM)$^{-1}$ and 2.40 mg (g DM)$^{-1}$ for spruce and birch, respectively (updated dataset of Merilä and Derome 2008). The mean pine needle N concentration in this dataset [1.27 mg (g DM)$^{-1}$] was assumed to generate LUE estimated for Hyytiälä.

Information about spatial distribution of species was obtained from the forest inventory data (NFI10 and NFI9), which was then scaled wall-to-wall at 500 m resolution using kriging (Härkönen *et al*. 2015). This information was further related to each 100 m simulation pixel by taking the species biomass weighted mean LUE estimate from the corresponding 500 m pixel.

We estimated the water holding capacity of soils of simulation cells (100 × 100 m) by first classifying soils to moist, typical mineral, and to thin drought prone soils, for which the calculations were made separately. We extracted areal proportions of soil types from the topographic map at 100 m resolution. Peatland areas were classified as moist soils where the effective pool of available soil water can be represented by a rooting depth of one metre. In reality, many peatland trees have shallow root layer, but peatlands collect water from the surroundings thus increasing the effective pool of available water. Soils with bare rock were classified drought-prone and assigned an effective rooting depth of 0.1 m. Any other areas were considered typical mineral (upland) soils with effective rooting depth of 0.5 m. Soil depth was used as a proxy for water holding capacity. These choices were based on expert judgment. This approach to classification assumes that soils can be coarsely classified to drought resistant, rarely drought vulnerable and drought prone soils. An area weighted mean value of soil depth in 100-m pixels was used in model runs.

Weather data

For production of weather data, we used a regional climate model REMO (Jacob and Podzun 1997, Jacob 2001), which employs CORINE land-cover data (Gao *et al*. 2015). The domain of the REMO run covered Fennoscandia with a resolution of 0.167°. ERA-Interim (Dee *et al*. 2011) re-analysis weather data of the European Centre for Medium-Range Weather Forecasts was used as lateral boundary for the large-scale atmospheric variables and surface

variables such as soil temperature, soil wetness and snow depth. The forward run covered the period from 1979 to 2011. An additional 10 year spin-up period was applied before the forward run to equilibrate slowly changing variables such as deep soil temperatures.

Throughout the atmosphere, the resolved climate variables are represented by a hybrid vertical coordinate system (Simmons and Burridge 1981). In addition to the resolved variables, the model produced parameterized 2-m air temperature and dew point temperature, as well as 10-m wind velocity for comparison with standard weather observations. In this work, we used these parameterized values for forcing JSBACH and PRELES.

JSBACH used the hourly REMO data for air temperature and specific humidity, wind speed, precipitation, short and long-wave radiation and potential shortwave radiation. Because these models operated in rotated latitude/longitude grid, no further processing of climatic data was applied in the off-line coupling of JSBACH and REMO.

For PRELES simulations, daily weather variables were linearly interpolated to 10 km resolution. For each simulation pixel at 100 m, PRELES used the closest 10-km grid point.

REMO-estimated weather for the years 2000–2011 was used in simulation comparisons. Gao *et al*. (2015) evaluated the weather data produced with REMO over the years 2001–2009 and found maximum daily air temperatures were overestimated in all seasons, the overestimation range from 2° to 4° in spring (Mar.–May) and from 1° to 3° in summer (Jun.–Aug.) and is less in autumn (Sep.–Nov.) and winter (Dec.–Feb.). The daily temperature ranges were underestimated by 1° to 5° by the model in all season except for winter (Dec.–Feb.). Precipitation was always overestimated by up to 90 mm per season.

GPP product of MODIS

We compared PRELES and JSBACH GPP predictions with MODIS remote sensing GPP predictions. Annual 1 × 1 km MODIS GPP products were provided by the MODIS GPP/NPP Project (MOD17) of the Numerical Terradynamic Simulation Group of the University of Montana (http://www.ntsg.umt.edu/project/mod17). The procedure for estimating MOD17 GPP algorithm has been described elsewhere (Running *et al*. 2004, Zhao *et al*. 2005). We aggregated the MODIS GPP and PRELES map products to correspond with the coarse spatial resolution of the JSBACH GPP product (16 × 16 km). We calculated the outcome of forest GPP of the MODIS product by utilizing a forest mask and an agriculture mask of the Corine Land Cover 2006 land cover product (25 m × 25 m) provided by the Finnish Environment Institute (SYKE) (http://wwwd3.ymparisto.fi/d3/Static_rs/spesific/corinelandcover.html). We assumed that the area-specific GPP of forests and agricultural land types are the same. We then calculated the difference between these different GPP products. Some of the MODIS pixels were clearly errornouos and had unrealistic GPP values (6500 g C m^{-2}). These were excluded from the analysis. All above GIS analyses were done with the Arcmap 10.0 program.

Case simulations

In addition to the annual GPP estimates, presented on maps, we prepared four simulations in order to compare the differences of model predictions by season and by species for one year of simulations (2006). For these purposes, we extracted PFT specific (coniferous and deciduous) GPP estimates for northern and southern Finland (67°51.6´N, 25°34.8´E; and 60°76´N, 23°54.8´E; respectively) from JSBACH simulations. In order to make comparable simulation with PRELES, we also extracted the corresponding weather data and annual mean LAI, which we converted into fraction of absorbed radiation as was earlier described for PRELES runs. For conifers, we ran PRELES with LUE parameters of pine, which hardly differed from that of spruce. For deciduous PFT, we used LUE parameters of birch. We present comparisons of GPP at medium water holding capacity soils in north and south.

Simulated site-level data were also compared with GPP determined for two eddy-covariance

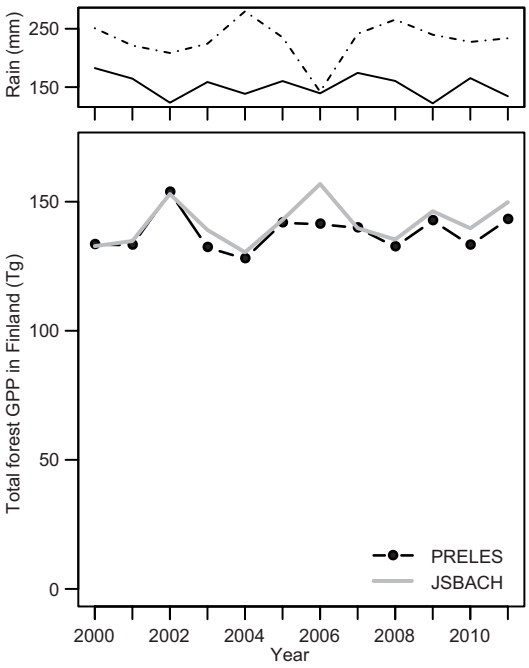

Fig. 1. Model estimated total GPP in Finland (bottom panel). Top panel shows mean precipitation in March–May (solid line) and in June–August (dash-dot line).

sites, one in northern Finland (Sodankylä), and one in southcentral Finland (Hyytiälä). We used the compilation of data presented in Peltoniemi *et al*. (2015), which was also used in the model calibration. Our case simulations in southern Finland were made for an area that had lower $f_{a\phi}$ (0.6) than Hyytiälä (0.8). Instead of presenting Hyytiälä data as they are, we multiplied its the daily GPP values buy a fraction $f_{a\phi,\text{case simulation}}/f_{a\phi,\text{Hyytiälä}}$ in order to obtain a 'measured' GPP for a hypothetical forest that has a smaller canopy than the forest in Hyytiälä.

Results

The estimates of annual GPP of Finland by JSBACH and PRELES were close to each other. PRELES estimated that the mean ± SD total forest GPP (2000–2011) was 137.9 ± 7.1 Tg a^{-1} and JSBACH estimated that it was 141.7 ± 8.3 Tg a^{-1} on the total forest areas of 18.9 million ha and 22.8 million ha, yielding 0.73 kg m^{-2} a^{-1} and 0.62 kg m^{-2} a^{-1}, respectively. Both models also showed similar inter-annual fluctuation of GPPs, the coefficient of variations (CV) of the estimates being 5.1% and 5.8% for PRELES and JSBACH, respectively (Fig. 1). A notable difference was in the year 2006, when there was little rain in June–August (Fig. 1) and PRELES predicted smaller GPP than JSBACH.

Large-scale spatial patterns of photosynthetising forest LAI were parallel in JSBACH and PRELES, but LAI of JSBACH was lower in the south and higher in the north as compared with that of PRELES (Fig. 2).

Overall, JSBACH and PRELES latitudinal distributions of mean GPPs matched (Fig. 3), and the predictions correlated adequately (r_P = 0.66) (*see* Fig. 4). Correlations between the grid GPP estimates of these two models and MODIS were weak. In northern Finland, GPP estimated with PRELES was smaller than that estimated with JSBACH (Figs. 4 and 5), which partially resulted from the smaller LAI used in PRELES than in JSBACH (Fig. 2). In southern Finland, especially in the southwestern corner of Finland, GPP estimated with PRELES was smaller, although LAI in southern Finland was higher. In the west of central Finland, JSBACH predicted smaller GPP than PRELES. Both differences can be partially attributed to the input data on soil water-holding capacity in PRELES. In southwestern Finland, forested pixels showed a high fraction of bare rock, which reduced the mean soil depth used by the model (Fig. 6), generating a moisture constraint on GPP that was the most pronounced during dry summer periods (Fig. 7). Areas in west-central Finland, on the other hand, had a high proportion of deep peatland soils (Fig. 6), which coincides with the areas for which PRELES estimated higher GPP than JSBACH (Fig. 5). GPP of MODIS was higher than the estimates of PRELES and JSBACH throughout the country (Figs. 3 and 5).

Site specific-model comparisons

In site-specific simulations, JSBACH predicted more variability in GPP of conifers than PRELES (Fig. 8). The level of GPP and its seasonal development were still similar for the conifers, and they were also consistent with the

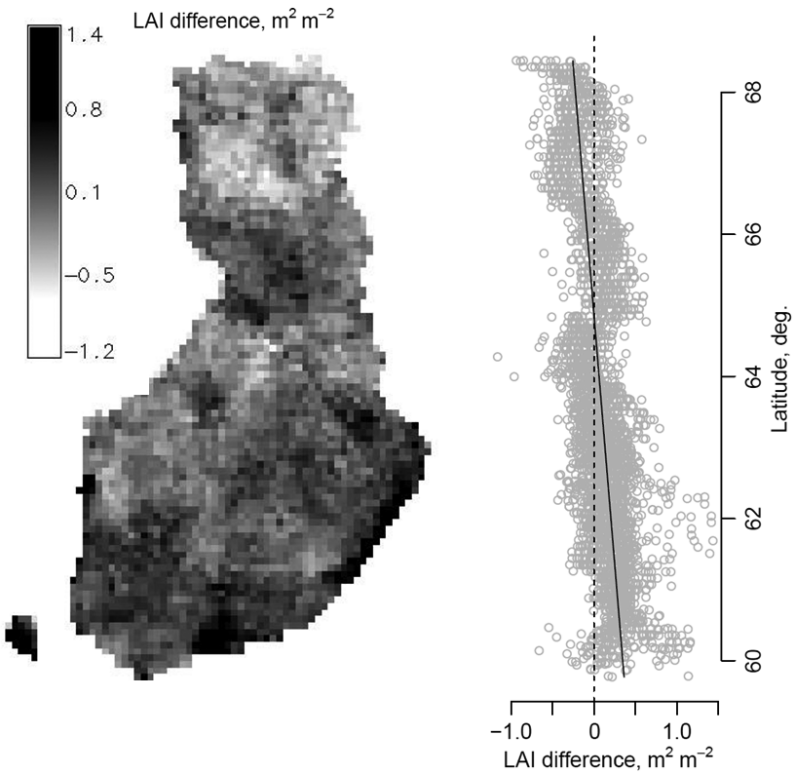

Fig. 2. The difference between the leaf area indices (one-sided) provided as inputs to PRELES and JSBACH, i.e. LAI_{PRELES} – LAI_{JSBACH}. The right-hand side of the figure shows the change in the LAI difference with latitude.

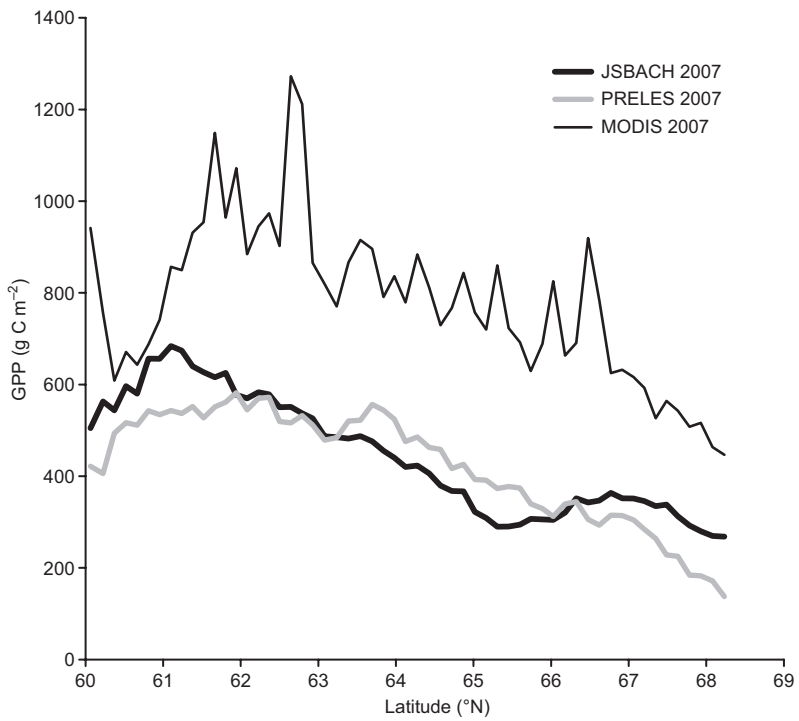

Fig. 3. Latitudinal change (moving average) in forest GPP predicted by PRELES, JSBACH and MODIS.

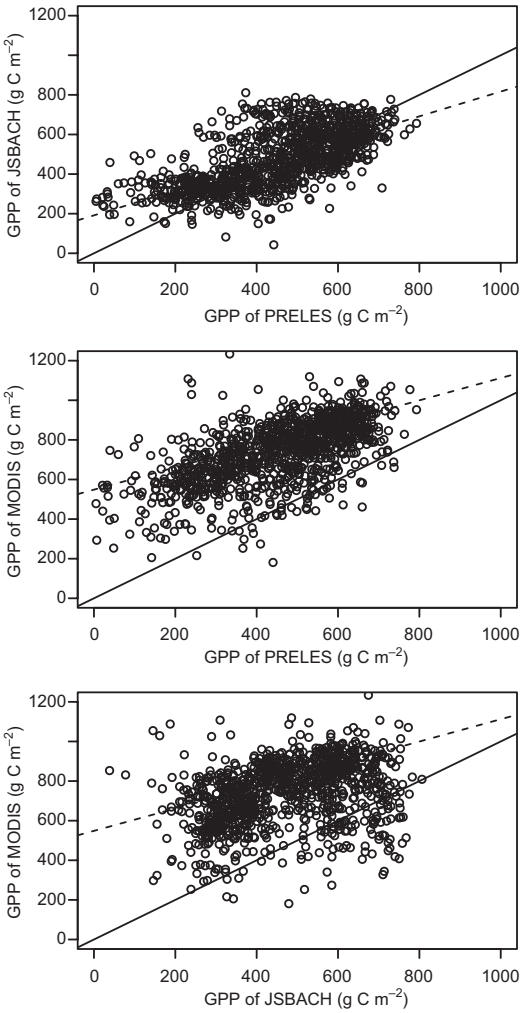

Fig. 4. One-to-one plots of mean GPP at unified-grid resolution (16 km). Solid line is 1:1 line. Dashed lines are the linear fits between the estimates. Pearson correlation coefficients between the estimate, from top to bottom, are r_P = 0.66 (95%CL = 0.63–0.69), r_P = 0.21 (95%CL = 0.15–0.26), r_P = 0.178 (95%CL = 0.12–0.23), respectively.

GPP determined for the eddy-covariance sites in northern (Sodankylä) and southcentral Finland (Hyytiälä). JSBACH predicted that GPP of conifers reached as high values as those of deciduous species, whereas PRELES predicted a higher maximum level for deciduous than coniferous species. Note also that the temporal pattern of the deciduous species is the same as in conifers in PRELES whereas JSBACH has a delay for the budburst of the deciduous species in spring.

Discussion

When data for model validation are sparse — a frequent situation with ecological models — it may be useful to compare models with each other, so as to find consistent patterns and to assess the causal chains leading to the simulated behaviour in the models. In this study, we compared two modelling approaches (PRELES and JSBACH) specifically adjusted for boreal conditions, with each other and with the generally available MODIS GPP product. The two former modelling approaches produced similar results regarding total production, temporal variability and latitudinal gradient of GPP. In the MODIS product, the total production was larger, while the overall latitudinal trend was similar (Fig. 3). The consistency between PRELES and JSBACH largely stems from the fact that their respective predictions for conifers coincided well with each other (and with data), as this group of species dominates the forests in Finland. Spatial differences were associated with the differences in input data on forests and soils, and how soil information was used by the models. The latitudinal trend of the GPP difference between JSBACH and PRELES can be explained by the PFT-specific phenology parameterization of JSBACH that generates higher LAI to northern Finland than is measured and modelled based on NFI data. The smaller GPP of PRELES in southern Finland, and higher in the west of central Finland, can be partially explained by the differences in soil information used by the models.

The GPP level difference between MODIS and the two other models could be partially reconciled by the inclusion of understorey vegetation in the models, as it contributes to the GPP of MODIS. Proportion of understorey GPP of forest total GPP is variable, and it has not been quantified at the level of Finland yet. The understorey GPP of a recently harvested Scots pine forest was 300 g C m^{-2}, while in a middle-aged (40-year-old) Scots pine stand in southcentral Finland it was 150 g C m^{-2} (Kolari *et al*. 2004, Kolari *et al*. 2006). The upper range of these predictions would almost close the gap between our models and MODIS, but it would likely be an overestimate, as clearcuts, young seedling stands, and harvested stands with some remain-

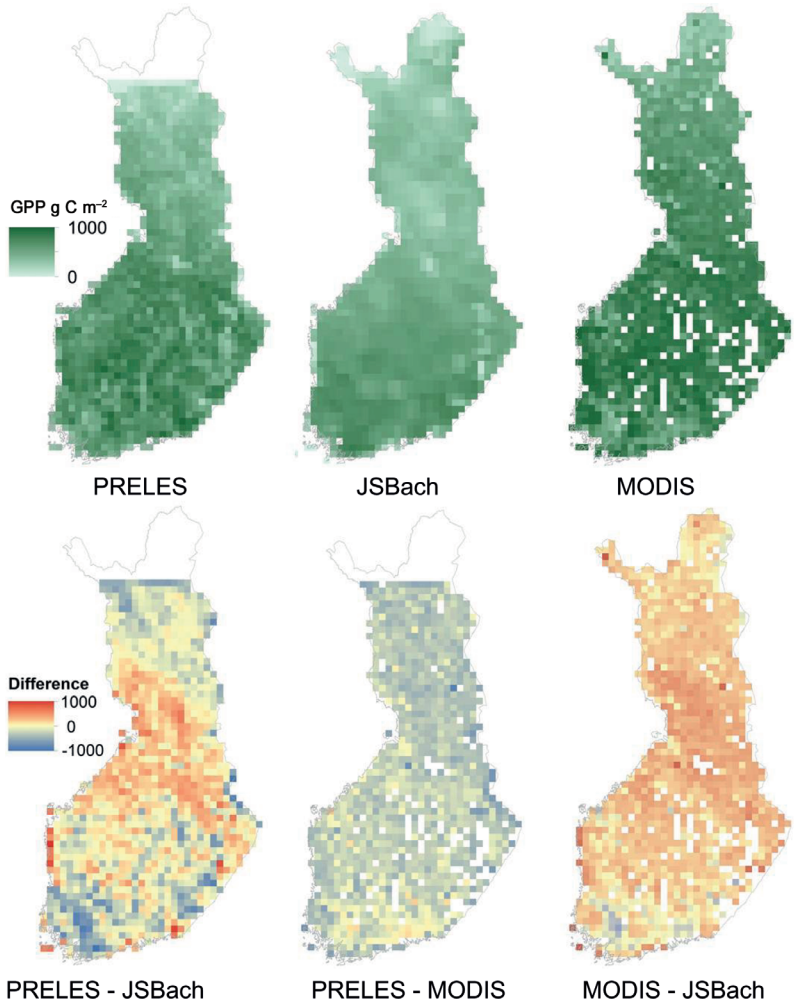

Fig. 5. GPP of forests predicted by PRELES, JSBACH, and MODIS for 2007. Bottom panels show the model differences.

ing and isolated seed trees only cover 20% of the area (Korhonen *et al*. 2013). Understorey is obviously an important part of GPP of boreal forests. Further studies on the role of the understorey in total national GPP are needed. Another issue that causes uncertainty in our comparison is the fact that the MODIS GPP product also sums up GPP of all land-cover types. We extracted forest GPP from the total GPP of MODIS using information on the area of forests and other land uses in the MODIS pixels, assuming equal GPP per unit of area in all land-cover classes. Uncertainty of MODIS-based forest GPP due to this operation decreases with latitude and longitude, i.e. in the direction where the fraction of forest coverage increases.

In JSBACH and PRELES the coefficient of variation (CV) of national total GPP was only 5%. There are few possibilities to relate this variation to GPP measurements at this scale, so we compared it with measured interannual variation of growth. In southern Finland, each of the main tree species (Norway spruce, Scots pine, birch) shows interannual variation in diameter growth with approximately 10% CV (interpreted from graphs of Henttonen 2000). For southern Finland alone, PRELES predicted CV of 7% (5.1% for northern Finland). At the country level, smaller CV could be expected also for the interannual variation of the mean diameter increment than for southern Finland alone. PRELES suggested that higher GPP variability in the south is

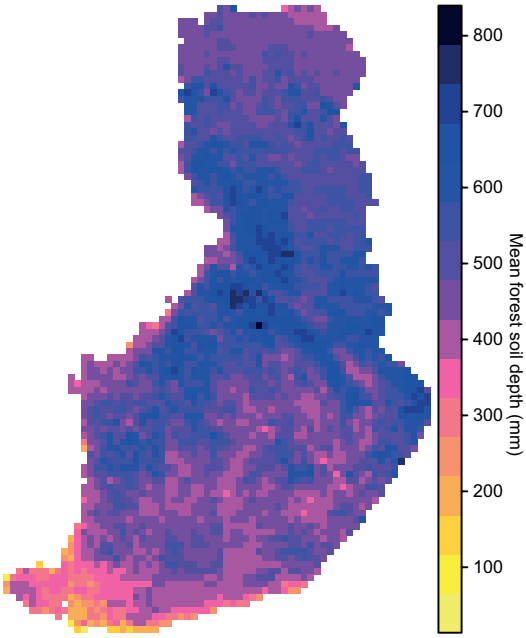

Fig. 6. Mean soil depth (mm) of forested area in PRELES simulations.

associated with soil moisture availability, especially in areas with shallow soils (not shown). Interestingly, it has been found that in southern Finland and Estonia, summer precipitation correlates with the increment variation of Scots pine (Henttonen 1984, Helama *et al*. 2005, Hordo *et al*. 2011), but in the north the growth is weakly associated with water (Lindholm 1996, Salminen *et al*. 2009, Korpela *et al*. 2011). In medium-deep soils, which were not as susceptible to drought reduction of GPP, it seems that the smaller CVs of model-predicted GPP than that of growth variation partially draws from the general model tendency to average variation. JSBACH and PRELES predicted GPP variation in site-level simulations (5%–8%) that was smaller than what we calculated using Hyytiälä eddy-covariance site data (13% for 1998–2009). One possible explanation for smaller variation in PRELES is the fact that the inter-annual or within-season variation in the leaf area was ignored. Leaf area varies, e.g., due to variation in litterfall (Starr *et al*. 2005) and in growth of new leafs and shoots. In JSBACH, on the other hand, LAI was related to current season temperature development, but the variation of maximum LAI was small across years (not shown), but CV still remained smaller. Further investigations of the relationship of GPP and growth variation are needed.

The role of water in controlling forest GPP and related processes has received little attention in the boreal zone but was incorporated in of JSBACH and PRELES. Recent predictions of climate change effects on tree growth, however, indicate a decline in tree species growth in southern Finland, which is attributed to soil water availability (Ge *et al*. 2011). Soil information plays a key role in such assessments,

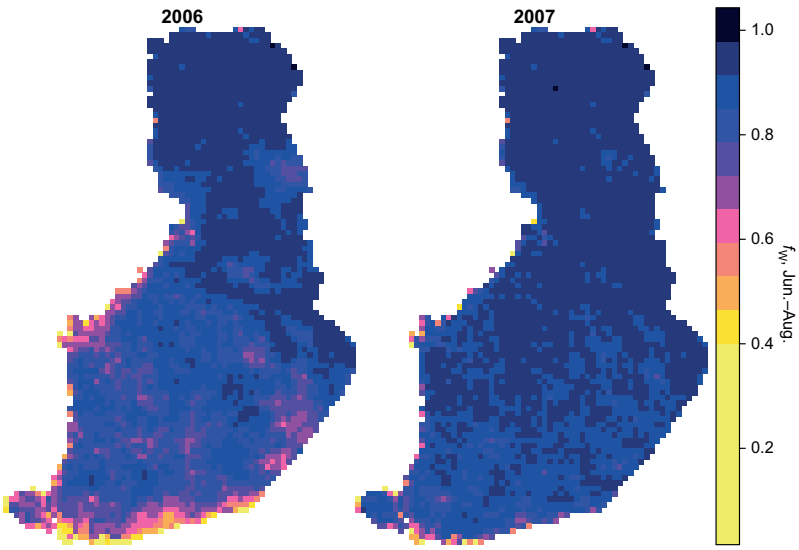

Fig. 7. Mean soil water constraint of PRELES ($f_W \in [0,1]$, is unitless and multiplies the potential GPP) in a dry (2006) and typical year (2007) during June–August.

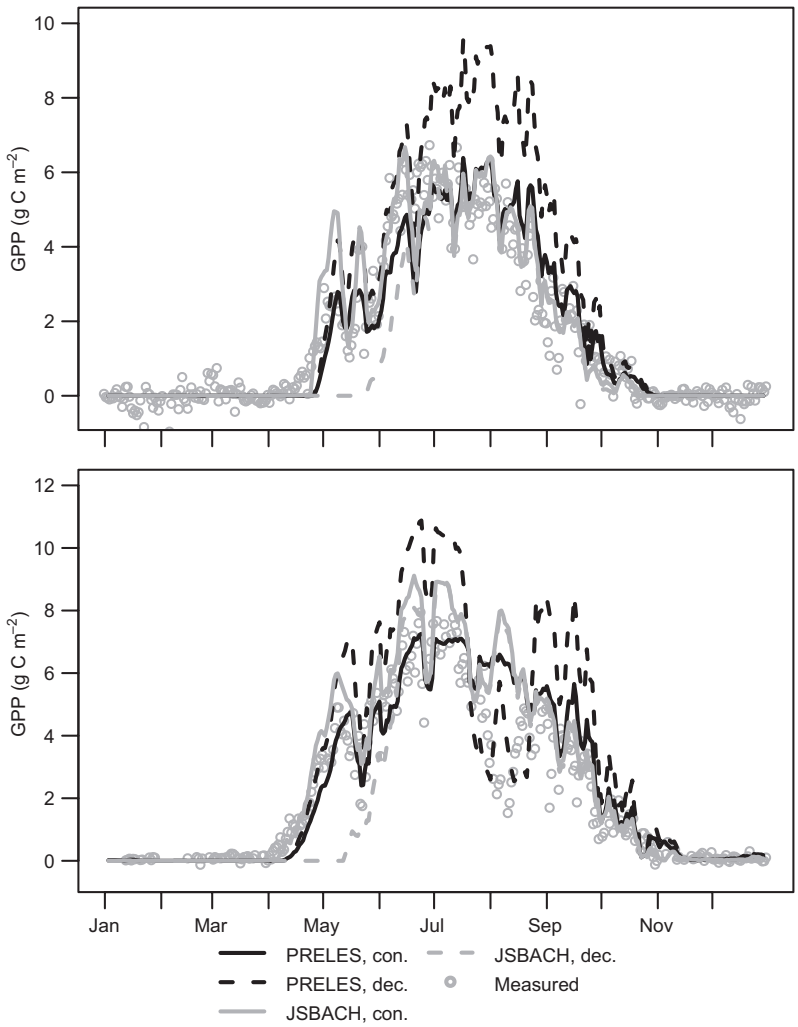

Fig. 8. Case simulations for the year 2006 in north (upper panel) and south (lower panel) Finland with parallel input data. Note that the eddy-covariance based GPP data from the southcentral site (Hyytiälä) were scaled to the same $f_{a\phi}$ that was simulated with the models for the region (*see* Material and methods). Also note that lower $f_{a\phi}$ used in the model simulations likely suppressed the prediction of Jul.–Aug. drought that is present in the scaled GPP data.

and in this sense it is interesting that the differences in simulated GPP between PRELES and JSBACH can be partially attributed to the soil properties (depth) used by the models. Soil water availability is largely dependent on small-scale topographic and edaphic variation, which create forest patches with shortage or excess of water. Such patchiness is not captured by global soil maps (FAO 1997) or even national-level soil map (Lilja *et al*. 2006). Therefore, in PRELES simulations, we used topographic map information appended with some assumptions of effective rooting depth; we accounted for the extreme cases only, the driest bare rock areas and the water-logged peatland forests, whereas other land was typical forest soil that is rarely drought prone. This classification is very coarse and obviously leaves room for improvement, but it could still catch most of the non-linear responses associated with soil water and GPP, given that the mean soil properties of the classes reflect the soil water effects well enough. Based on this approach, we found a tendency that the shallowest soils (with forests) were in southern Finland, where also much of the fertile land is in active use in agriculture. Interestingly, climate scenarios also predict increases in summer soil moisture deficit in southern Finland (Carter *et al*. 2005), which means that this combination could make southern forests susceptible to drought. It is also noteworthy that we did not find much water-induced variation in national total forest

GPP in JSBACH, which could either imply that JSBACH is less sensitive to water or that the combination of coarse level global soil maps texture data and PFT specific parameterization of plant available water used in JSBACH does not capture the drought stemming from local soil conditions.

Issues related to soil water-holding capacity and rooting zone remain enigmatic and their consequences are hard to evaluate at a large scale. Therefore, simplifications are of great interest, which is probably among the reasons why drought-index approaches have become popular (*see* e.g. Palmer 1965, Vicente-Serrano *et al*. 2009). Similar type of temporally-scaled indices can also be derived using ecosystem models that often predict rooting depth soil water without accounting for lateral water fluxes (Muukkonen *et al*. 2015). Simple non-spatial water balance estimation methods could also be merged with topographic information (e.g. Murphy *et al*. 2009) in order to account better for lateral slow processes of water accumulation.

It seems that JSBACH and PRELES compare well with data and each other when predicting GPP of conifers, which is not a surprise given the eddy-covariance data sets available for calibration in Finland (Peltoniemi *et al*. 2015). In contrast, GPP of deciduous species did not show equally good agreement between the models. Both models would benefit from better information about the development of leaves and their photosynthetic capacity (or LUE), and their maximum attainable levels. Those were studied elsewhere (Linkosalo *et al*. 2008), so in the near future we expect to improve these model parts. This has, however, a relatively small effect on the country level GPP total, due to the fact that deciduous trees are only 25% of the growing stock (Korhonen *et al*. 2013). Based on this percentage and our case simulations for deciduous species, we estimated that GPP accumulated in PRELES simulations during the spring (Apr.–15 Jun.) when GPP of JSBACH was zero or low adds 4% to national total GPP.

In spite of the numerous potential improvements of the models, the model estimates of GPP (137.9, and 141.7 Tg, PRELES and JSBACH, respectively) were in reasonable agreement with the national forest green-house gas (ghg) inventory estimate (167.5 Tg) that was derived from the forest inventory records (Statistics Finland 2012) and the data used in these calculations (A. Lehtonen pers. comm.). The key aspect of this comparison is the equivalence of GPP obtained with models utilizing CO_2 flux data in their calibrations and GPP derived using independent biomass stock change, turnover and removals information (Liski *et al*. 2006). Uncertainties remain in all estimates, and in the conversion of NPP to GPP. It has been estimated that CV of annual total litter production (incl. natural losses and harvests) in Finland is 12%–13% (Peltoniemi *et al*. 2006), while the national inventory report (Statistics Finland 2012) mentions that CV of biomass stock increment is 8%. Using these estimates and the estimates of litter and biomass increment, one can estimate an upper limit of CV of inventory-based NPP (in case of uncorrelated litter and increment uncertainties) that is 8.1%. We further assumed that GPP is twice the inventory-derived NPP (net primary production), which is a rough estimation, but which does have empirical support (Waring *et al*. 1998). It is notable that the forest area simulated by PRELES excluded the northernmost part of Finland, and some of the cloud-covered pixels elsewhere leading to an area smaller than the inventories. Better correspondence of areas would reduce the difference between GPP of PRELES and inventory further, although it is not likely to quite close the gap.

JSBACH and PRELES produced similar estimates of GPP at the country level, they showed similar spatial trends, and they compare well with measured data and each other in site level simulations. Furthermore, it seems that differences with the MODIS GPP product could be partially, although not completely, explained by understorey vegetation. Our models also produced estimates of GPP in fair agreement with the estimates derived from the data used in the reporting of national forest greenhouse gas inventory to the UNFCCC. This is remarkable as all these estimates are based on different approaches, and calibration data sets, PRELES currently calibrated with eddy-covariance data from only two sites. JSBACH parameters, on the other hand, draw from generic PFT-parameters that originate outside the study region. Consist-

ently with previous studies (e.g. Duursma *et al*. 2009) these findings seem to imply that the GPP process is highly generalizable, and that its calibration does not require extensive data sets. Some differences still remained in the model estimates. PRELES produced more variability in GPP both spatially and temporally. The spatial variability results firstly, from the fine resolution differences in the LAI input and its latitudinal gradient, as the overall levels of LAI coincided, and secondly from the differences in the soil data used in soil water models, and likely also due to the model sensitivities to soil water. Predicting water effects on ecosystem fluxes, and modelling the consequent year-to-year effects on GPP remains an important future research task.

Acknowledgements: This study was produced in projects Climforisk (EU Life+ project LIFE09 ENV/FI/000571 Climate change induced drought effects on forest growth and vulnerability) and SnowCarbo (EU Life+, LIFE07 ENV/FIN/000133). TT was funded by Acedemy of Finland (grant no. 266803). We thank Aleksi Lehtonen and Matti Katila for discussions. We acknowledge MPI-M for the JSBACH code. We thank Christian Reick and Sönke Zaehle for discussions and advice in using JSBACH. This study was conducted in the frame of COST STReESS (FP1106).

References

Bellassen V., Le Maire G., Dhôte J.F., Ciais P. & Viovy N. 2010. Modelling forest management within a global vegetation model — Part 1: Model structure and general behaviour. *Ecol. Model.* 221: 2458–2474.

Bonan G.B. 2008. Forests and climate change: forcings, feedbacks, and the climate benefits of forests. *Science* 320: 1444–1449.

Brovkin V., Claussen M., Driesschaert E., Fichefet T., Kicklighter D., Loutre M.F., Matthews H.D., Ramankutty N., Schaeffer M. & Sokolov A. 2006. Biogeophysical effects of historical land cover changes simulated by six Earth system models of intermediate complexity. *Clim. Dynam.* 26: 587–600.

Büttner G. & Kosztra B. 2007. *CLC2006 technical guidelines*. Technical Report 17, European Environment Agency.

Carter T.R., Jylhä K., Perrels A., Fronzek S. & Kankaanpää S. 2005. *FINADAPT scenarios for the 21st century. Alternative futures for considering adaptation to climate change in Finland*. FINADAPT Working Paper 2.

Dee D.P., Uppala S.M., Simmons A.J., Berrisford P., Poli P., Kobayashi S., Andrae U., Balmaseda M.A., Balsamo G., Bauer P., Bechtold P., Beljaars A.C.M., van de Berg L., Bidlot J., Bormann N., Delsol C., Dragani R., Fuentes M., Geer A.J., Haimberger L., Healy S.B., Hersbach H., Hólm E.V., Isaksen L., Kållberg P., Köhler M., Matricardi M., McNally A.P., Monge-Sanz B.M., Morcrette J.-J., Park B.-K., Peubey C., de Rosnay P., Tavolato C., Thépaut J.-N. & Vitart F. 2011. The ERA-Interim reanalysis: configuration and performance of the data assimilation system. *Q. J. R. Meteorol. Soc.* 137: 553–597.

Duursma R.A., Kolari P., Perämäki M., Pulkkinen M., Mäkelä A., Nikinmaa E., Hari P., Aurela M., Berbigier P., Bernhofer C., Grünwald T., Loustau D., Mölder M., Verbeeck H. & Vesala T. 2009. Contributions of climate, leaf area index and leaf physiology to variation in gross primary production of six coniferous forests across Europe: a model-based analysis. *Tree Physiol.* 29: 621–639.

EC 2007. *Directive 2007/2/EC of the European Parliament and of the Council of 14 March 2007 establishing an Infrastructure for Spatial Information in the European Community (INSPIRE)*. Official Journal of the European Union 108(50).

FAO 1979. *Soil map of the world*, vol. 5. UNESCO, Paris.

Farquhar G.D., Caemmerer S. & Berry J. 1980. A biochemical model of photosynthetic CO_2 assimilation in leaves of C3 species. *Planta* 149: 78–90.

Fix E. & Hodges J.L.Jr. 1951. *Discriminatory analysis-nonparametric discrimination: consistency properties*. Report number 4, USAF School of Aviation Medicine, Randolph Field, Texas.

Friedlingstein P., Cox P., Betts R., Bopp L., von Bloh W., Brovkin V., Cadule P., Doney S., Eby M., Fung I., Bala G., John J., Jones C., Joos F., Kato T., Kawamiya M., Knorr W., Lindsay K., Matthews H.D., Raddatz T., Rayner P., Reick C., Roeckner E., Schnitzler K., Schnur R., Strassmann K., Weaver A.J., Yoshikawa C. & Zeng N. 2006. Climate–carbon cycle feedback analysis: results from the C4MIP model intercomparison. *J. Climate* 19: 3337–3353.

Gao Y., Weiher S., Markkanen T., Pietikäinen J.-P., Gregow H., Henttonen H.M., Jacob D. & Laaksonen A. 2015: Implementation of the CORINE land use classification in the regional climate model REMO. *Boreal Env. Res.* 20: 261–282.

Ge Z., Kellomäki S., Peltola H., Zhou X., Wang K. & Väisänen H. 2011. Impacts of changing climate on the productivity of Norway spruce dominant stands with a mixture of Scots pine and birch in relation to water availability in southern and northern Finland. *Tree Physiol.* 31: 323–338.

Hagemann S. 2002. *An improved land surface parameter dataset for global and regional climate models*. Report No. 336, Max Planck Institute for Meteorology.

Hagemann S. & Stacke T. 2015. Impact of the soil hydrology scheme on simulated soil moisture memory. *Clim. Dynam.* 44: 1731–1750.

Härkönen S., Pulkkinen M., Duursma R. & Mäkelä A. 2010. Estimating annual GPP, NPP and stem growth in Finland using summary models. *For. Ecol. Manage.* 259: 524–533.

Härkönen S., Lehtonen A., Eerikäinen K., Peltoniemi M. & Mäkelä A. 2011. Estimating forest carbon fluxes for large regions based on process-based modelling, NFI

data and Landsat satellite images. *For. Ecol. Manage.* 262: 2364–2377.

Härkönen S., Lehtonen A., Manninen T., Tuominen S. & Peltoniemi, M. 2015: Estimating forest leaf area index using satellite images: comparison of *k*-NN based Landsat-NFI LAI with MODIS-RSR based LAI product for Finland. *Boreal Env. Res.* 20: 181–195.

Hasenauer H., Petritsch R., Zhao M., Boisvenue C. & Running S.W. 2012. Reconciling satellite with ground data to estimate forest productivity at national scales. *For. Ecol. Manage.* 276: 196–208.

Helama S., Lindholm M., Meriläinen J., Timonen M. & Eronen M. 2005. Multicentennial ring-width chronologies of Scots pine along a north-south gradient across Finland. *Tree-Ring Res.* 61: 21–32.

Henttonen H. 1984. The dependence of annual ring indices on some climatic factors. *Acta For. Fennica* 186: 1–23.

Henttonen H. 2000. Growth variation. In: Mälkönen E. (ed.), *Forest condition in a changing environment — the Finnish case*, Forestry Sciences vol. 65, Kluwer Academic Publishers, pp. 25–32.

Hordo M., Henttonen H., Mäkinen H., Helama S. & Kiviste A. 2011. Annual growth variation of Scots pine in Estonia and Finland. *Baltic For.* 17: 35–49.

Jacob D. 2001. A note to the simulation of the annual and inter-annual variability of the water budget over the Baltic Sea drainage basin. *Meteorol. Atmos. Phys.* 77: 61–73.

Jacob D. & Podzun R. 1997. Sensitivity studies with the regional climate model REMO. *Meteorol. Atmos. Phys.* 63: 119–129.

Jung M., Reichstein M., Margolis H.A., Cescatti A., Richardson A.D., Arain M.A., Arneth A., Bernhofer C., Bonal D., Chen J., Gianelle D., Gobron N., Kiely G., Kutsch W., Lasslop G., Law B.E., Lindroth A., Merbold L., Montagnani L., Moors E.J., Papale D., Sottocornola M., Vaccari F. & Williams C. 2011. Global patterns of land-atmosphere fluxes of carbon dioxide, latent heat, and sensible heat derived from eddy covariance, satellite, and meteorological observations. *J. Geophys. Res.* 116: G00J07, doi:10.1029/2010JG001566.

Kattge J., Knorr W., Raddatz T. & Wirth C. 2009. Quantifying photosynthetic capacity and its relationship to leaf nitrogen content for global-scale terrestrial biosphere models. *Global Change Biol.* 15: 976–991.

Kilkki P. & Päivinen R. 1987. Reference sample plots to combine field measurements and satellite data in forest inventory. In: *Research Notes* 19, Department of Forest Mensuration and Management, University of Helsinki, pp. 209–215.

Knorr W. 1997. *Satellite remote sensing and modelling of the global CO_2 exchange of land vegetation: a synthesis study*. Examensarbeit, Max-Planck-Institut für Meteorologie.

Kolari P., Pumpanen J., Rannik Ü, Ilvesniemi H., Hari P. & Berninger F. 2004. Carbon balance of different aged Scots pine forests in Southern Finland. *Global Change Biol.* 10: 1106–1119.

Kolari P., Pumpanen J., Kulmala L., Ilvesniemi H., Nikinmaa E., Grönholm T. & Hari P. 2006. Forest floor vegetation plays an important role in photosynthetic production of boreal forests. *For. Ecol. Manage.* 221: 241–248.

Korhonen K.T., Ihalainen A., Viiri H., Heikkinen J., Henttonen H.H., Hotanen J., Mäkelä H., Nevalainen S. & Pitkänen J. 2013. Suomen metsät 2004–2008 ja niiden kehitys 1921–2008. *Metsätieteen aikakauskirja* 3: 269–608.

Korpela M., Nöjd P., Hollmén J., Mäkinen H., Sulkava M. & Hari P. 2011. Photosynthesis, temperature and radial growth of Scots pine in northern Finland: identifying the influential time intervals. *Trees — Struct. Funct.* 25: 323–332.

Lilja H., Uusitalo R., Yli-Halla M., Nevalainen R., Väänänen T. & Tamminen P. 2006. *Suomen maannostietokanta: Maannoskartta 1:250 000 ja maaperän ominaisuuksia*. MTT:n selvityksiä 114.

Lindholm M. 1996. *Reconstruction of past climate from ring-width chronologies of Scots pine (Pinus sylvestris L.) at the northern limit in Fennoscandia*. Ph.D. thesis University of Joensuu.

Linkosalo T., Lappalainen H.K. & Hari P. 2008. A comparison of phenological models of leaf bud burst and flowering of boreal trees using independent observations. *Tree Physiol.* 28: 1873–1882.

Liski J., Lehtonen A., Peltoniemi M., Eggers T., Muukkonen P. & Mäkipää R. 2006. Carbon accumulation in Finland's forests 1922–2004 — an estimate obtained by combination of forest inventory data with modelling of biomass, litter and soil. *Ann. For. Sci.* 63: 687–697.

Mäkelä A., Pulkkinen M., Kolari P., Lagergren F., Berbigier P., Lindroth A., Loustau D., Nikinmaa E., Vesala T. & Hari P. 2008. Developing an empirical model of stand GPP with the LUE approach: analysis of eddy covariance data at five contrasting conifer sites in Europe. *Global Change Biol.* 14: 92–108.

Merilä P. & Derome J. 2008. Relationships between needle nutrient composition in Scots pine and Norway spruce stands and the respective concentrations in the organic layer and in percolation water. *Boreal Env. Res.* 13: 35–47.

Monteith J.L. & Moss C.J. 1977. Climate and the efficiency of crop production in Britain [and discussion]. *Phil. Trans. Royal Soc. London B* 281: 277–294.

Murphy P.N.C., Ogilvie J. & Arp P. 2009. Topographic modelling of soil moisture conditions: a comparison and verification of two models. *Eur. J. Soil. Sci.* 60: 94–109.

Muukkonen P., Nevalainen S., Lindgren M. & Peltoniemi M. 2015: Spatial occurrence of drought-associated damages in Finnish boreal forests: results from forest condition monitoring and GIS analysis. *Boreal Env. Res.* 20: 172–180.

Olson J. 1994a. *Global ecosystem framework-definitions*. Internal Report 37, USGS EROS Data Center, Sioux Falls, SD.

Olson J. 1994b. *Global ecosystem framework-translation strategy*. Internal Report 39, USGS EROS Data Center, Sioux Falls, SD.

Palmer W.C. 1965. *Meteorological drought*. US Department of Commerce, Weather Bureau, Washington, DC.

Peltoniemi M., Palosuo T., Monni S. & Mäkipää R. 2006. Factors affecting the uncertainty of sinks and stocks of

carbon in Finnish forests soils and vegetation. *For. Ecol. Manage*. 232: 75–85.

Peltoniemi M., Pulkkinen M., Aurela M., Pumpanen J., Kolari P. & Mäkelä A. 2015: A semi-empirical model of boreal-forest gross primary production, evapotranspiration, and soil water — calibration and sensitivity analysis. *Boreal Env. Res*. 20: 151–171.

Peltoniemi M., Pulkkinen M., Kolari P., Duursma R.A., Montagnani L., Wharton S., Lagergren F., Takagi K., Verbeeck H., Christensen T., Vesala T., Falk M., Loustau D. & Mäkelä A. 2012. Does canopy mean nitrogen concentration explain variation in canopy light use efficiency across 14 contrasting forest sites? *Tree Physiol*. 32: 200–218.

Pongratz J., Reick C.H., Raddatz T. & Claussen M. 2009. Effects of anthropogenic land cover change on the carbon cycle of the last millennium. *Global Biogeochem. Cycles* 23: GB4001, doi:10.1029/2009GB003488.

Pongratz J., Reick C.H., Raddatz T. & Claussen M. 2010. Biogeophysical versus biogeochemical climate response to historical anthropogenic land cover change. *Geophys. Res. Lett*. 37: L08702, doi:10.1029/2010GL043010.

Poso S. 1972. A method for combining photo and field samples in forest inventory. *Communicationes Instituti Forestalis Fenniae* 76: 1–133.

Prentice I.C., Cramer W., Harrison S.P., Leemans R., Monserud R.A. & Solomon A.M. 1992. Special paper: A Global biome model based on plant physiology and dominance, soil properties and climate. *J. Biogeogr.* 19: 117–134.

Raddatz T.J., Reick C.H., Knorr W., Kattge J., Roeckner E., Schnur R., Schnitzler K., Wetzel P. & Jungclaus J. 2007. Will the tropical land biosphere dominate the climate-carbon cycle feedback during the twenty-first century? *Climate Dynamics* 29: 565–574.

Reick C.H., Raddatz T., Brovkin V. & Gayler V. 2013. Representation of natural and anthropogenic land cover change in MPI-ESM. *J. Adv. Model Earth Syst*. 5: 459–482.

Repola J. 2009. Biomass equations for Scots pine and Norway spruce in Finland. *Silva Fenn*. 43: 625–647.

Running S.W., Nemani R.R., Heinsch F.A., Zhao M., Reeves M. & Hashimoto H. 2004. A continuous satellite-derived measure of global terrestrial primary production. *Bioscience* 54: 547–560.

Salminen H., Jalkanen R. & Lindholm M. 2009. Summer temperature affects the ratio of radial and height growthof Scots pine in northern Finland. *Ann. For. Sci*. 66: 1–9.

Schulze E., Kelliher F.M., Korner C., Lloyd J. & Leuning R. 1994. Relationships among maximum stomatal conductance, ecosystem surface conductance, carbon assimilation rate, and plant nitrogen nutrition: a global ecology scaling exercise. *Annu. Rev. Ecol. Syst*. 25: 629–660.

Sellers P.J. 1985. Canopy reflectance, photosynthesis and transpiration. *Int. J. Remote Sens*. 6: 1335–1372.

Simmons A.J. & Burridge D.M. 1981. An energy and angular-momentum conserving vertical finite-difference scheme and hybrid vertical coordinates. *Mon. Wea. Rev.* 109: 758–766.

Starr M., Saarsalmi A., Hokkanen T., Merilä P. & Helmisaari H. 2005. Models of litterfall production for Scots pine (*Pinus sylvestris* L.) in Finland using stand, site and climate factors. *For. Ecol. Manage*. 205: 215–225.

Statistics Finland 2012. Greenhouse gas emissions of Finland, National Inventory Report under the UNFCCC and the Kyoto Protocol.

Stevens B., Giorgetta M., Esch M., Mauritsen T., Crueger T., Rast S., Salzmann M., Schmidt H., Bader J., Block K., Brokopf R., Fast I., Kinne S., Kornblueh L., Lohmann U., Pincus R., Reichler T. & Roeckner E. 2013. Atmospheric component of the MPI-M earth system model: ECHAM6. *J. Adv. Model Earth Syst*. 5: 146–172.

Tomppo E. 1990. Satellite image-based national forest inventory of Finland. *The Photogrammetric Journal of Finland* 12: 115–120.

Tomppo E., Haakana M., Katila M. & Peräsaari J. 2008. *Multi-source national forest inventory — methods and application*. Managing Forest Ecosystems 18, Springer.

Tomppo E., Katila M., Mäkisara K. & Peräsaari J. 2012. The multi-source National Forest Inventory of Finland — methods and results 2007. *Working Papers of the Finnish Forest Research Institute* 227: 1–233.

Tuominen S., Eerikäinen K., Schibalski A., Haakana M. & Lehtonen A. 2010. Mapping biomass variables with a multi-source forest inventory technique. *Silva Fenn*. 44: 109–119.

Veroustraete F., Sabbe H. & Eerens H. 2002. Estimation of carbon mass fluxes over Europe using the C-Fix model and Euroflux data. *Remote Sens. Environ*. 83: 376–399.

Vicente-Serrano S.M., Beguería S. & López-Moreno J.I. 2009. A multiscalar drought index sensitive to global warming: the standardized precipitation evapotranspiration index. *J. Climate* 23: 1696–1718.

VMI 2008. *Valtakunnan metsien 10. inventointi (VMI10) - Maastotyön ohjeet 2008, koko Suomi*. Metsäntutkimuslaitos, Helsinki.

Waring R.H., Landsberg J.J. & Williams M. 1998. Net primary production of forests: a constant fraction of gross primary production? *Tree Physiol*. 18: 129–134.

Williams M., Richardson A.D., Reichstein M., Stoy P.C., Peylin P., Verbeeck H., Carvalhais N., Jung M., Hollinger D.Y., Kattge J., Leuning R., Luo Y., Tomelleri E., Trudinger C.M. & Wang Y.-P. 2009. Improving land surface models with FLUXNET data. *Biogeosciences* 6: 1341–1359.

Wullschleger S.D. 1993. Biochemical limitations to carbon assimilation in C3 plants — a retrospective analysis of the A/Ci curves from 109 species. *J. Exp. Bot*. 44: 907–920.

Xiao X., Zhang Q., Braswell B., Urbanski S., Boles S., Wofsy S., Moore B.III & Ojima D. 2004. Modeling gross primary production of temperate deciduous broadleaf forest using satellite images and climate data. *Remote Sens. Environ*. 91: 256–270.

Ylitalo E. 2012. *Metsätilastollinen vuosikirja 2012 — Skogsstatistisk årsbok*. Metsäntutkimuslaitos, Vantaa.

Zhao M., Running S.W. & Nemani R.R. 2006. Sensitivity of Moderate Resolution Imaging Spectroradiometer (MODIS) terrestrial primary production to the accuracy

of meteorological reanalyses. *J. Geophys. Res.* 111: G01002, doi:10.1029/2004JG000004.

Zhao M., Heinsch F.A., Nemani R.R. & Running S.W. 2005. Improvements of the MODIS terrestrial gross and net primary production global data set. *Remote Sens. Environ.* 95: 164–176.